J. Biochem. 2011;149(4):487–494 doi:10.1093/jb/mvr009

JB THE JOURNAL OF BIOCHEMISTRY

Structural basis of species differences between human and experimental animal CYP1A1s in metabolism of 3,3′,4,4′,5-pentachlorobiphenyl

Received September 21, 2010; accepted December 27, 2010; published online January 22, 2011

Kiyoshi Yamazaki[1], Motoharu Suzuki[1,2], Toshimasa Itoh[3], Keiko Yamamoto[3], Miki Kanemitsu[4], Chisato Matsumura[2], Takeshi Nakano[2], Toshiyuki Sakaki[5], Yasuo Fukami[4,6], Hiromasa Imaishi[1,4,6] and Hideyuki Inui[1,4,6,*]

[1]Graduate School of Agricultural Science, Kobe University, 1-1 Rokkodai-cho, Nada-ku, Kobe, Hyogo 657-8501; [2]Hyogo Prefectural Institute of Environmental Sciences, 3-1-27 Yukihira-cho, Suma-ku, Kobe, Hyogo 654-0037; [3]Laboratory of Drug Design and Medicinal Chemistry, Showa Pharmaceutical University, 3-3165, Higashi-tamagawagakuen, Machida, Tokyo 194-8543; [4]Graduate School of Science and Technology, Kobe University, 1-1 Rokkodai-cho, Nada-ku, Kobe, Hyogo 657-8501; [5]Biotechnology Research Center, Faculty of Engineering, Toyama Prefectural University, 5180 Kurokawa, Imizu, Toyama 939-0398; and [6]Research Center for Environmental Genomics, Kobe University, 1-1 Rokkodai-cho, Nada-ku, Kobe, Hyogo 657-8501, Japan

*Hideyuki Inui, Research Center for Environmental Genomics, Kobe University, 1-1 Rokkodai-cho, Nada-ku, Kobe, Hyogo 657-8501, Japan. Tel: +81 78 803 5863, Fax: +81 78 803 5863, email: hinui@kobe-u.ac.jp

Coplanar polychlorinated biphenyls included in dioxin-like compounds are bio-accumulated and adversely affect wildlife and human health. Although many researchers have studied the metabolism of PCBs, there have been few reports of the *in vitro* metabolism of 3,3′,4,4′,5-pentachlorobiphenyl (PCB126), despite the fact that it has the highest toxicity among PCB congeners. Cytochrome P450 (CYP) 1A1 proteins can metabolize some dioxins and PCBs by hydroxylation, but the activities of human and rat CYP1A1 proteins are very different. The mechanism remains unclear. From our results, rat CYP1A1 metabolized PCB126 into 4-OH-3,3′,4′,5-tetrachlorobiphenyl and 4-OH-3,3′,4′,5,5′-pentachlorobiphenyl, but human CYP1A1 did not metabolize. Homology models of the two CYP proteins, and docking studies, showed that differences in the amino acid residues forming their substrate-binding cavities led to differences in the size and shape of the cavities; only the cavity of rat CYP1A1 allowed PCB126 close enough to the haem to be metabolized. Comparison of the amino acid residues of other mammalian CYP1A1 proteins suggested that rats have a unique metabolism of xenobiotics. Our results suggest that it is necessary to be careful in human extrapolation of toxicity data estimated by using the rat as an experimental animal, especially in the case of compounds metabolized by CYP1A1.

Keywords: cytochrome P450/docking approach/homology modelling/persistent organic pollutants/polychlorinated biphenyl.

Abbreviations: AhR, aryl hydrocarbon receptor; CYP, cytochrome P450; HRGC/HRMS, high-resolution gas chromatography/high-resolution mass spectrometry; MeO-PeCB, methylated mono hydroxylated pentachlorobiphenyl; MeO-TeCB, methylated mono hydroxylated tetrachlorobiphenyl; OH-PCB, hydroxylated polychlorinated biphenyl; OH-PeCB, hydroxylated pentachlorobiphenyl; OH-TeCB, hydroxylated tetrachlorobiphenyl; PCB, polychlorinated biphenyl; PCB126, 3,3′,4,4′,5-pentachlorobiphenyl; PCDD, polychlorinated dibenzo-*p*-dioxin; PCDF, polychlorinated dibenzofuran; POPs, persistent organic pollutants; SIM, selective ion monitoring; TCDD, tetrachlorodibenzo-*p*-dioxin; TeCB, tetrachlorobiphenyl; TEF, toxic equivalence factor; TriCDD, trichlorodibenzo-*p*-dioxin.

Polychlorinated biphenyls (PCBs) are composed of 209 structurally related congeners, and their structures consist of two connected benzene rings and 1–10 chlorine atoms. Although PCBs were used widely in many common products and in industrial applications such as electrical insulating fluids and heat-exchange fluids, increased understanding of the risks to the environment and human health has caused the production and use of PCBs to be restricted in most countries.

Because of their chemical stability and resistance to degradation, there are many areas polluted with PCBs globally, and PCBs remain problematic compounds. Particularly problematic are PCBs with coplanarity, called coplanar PCBs, which are dioxin-related compounds with structures similar to those of polychlorinated dibenzo-*p*-dioxins (PCDDs) and polychlorinated dibenzofurans (PCDFs); coplanar PCBs are classified as persistent organic pollutants (POPs). The Stockholm Convention on POPs prohibits and limits their production, use, import and export (http://chm.pops.int/default.aspx), and governments need to try to reduce their release into the environment.

In animal studies, PCBs show carcinogenicity and developmental, neuronal and reproductive toxicities.

The toxicology of coplanar PCBs in mammals is similar to those of PCDDs and PCDFs and is thus largely related to the action of the aryl hydrocarbon receptor (AhR). The AhR is a ligand-activated transcription factor. It regulates organ development and detoxification of xenobiotics by upregulating detoxification enzymes such as cytochrome P450 (CYP, P450) species (*1*).

P450 enzymes play important physiological roles in the detoxification of xenobiotics and the biosynthesis of endogenous compounds. Among them, hepatic drug-metabolizing P450s belonging to P450 families 1, 2 and 3 are the principal enzymes involved in the biotransformation of xenobiotics to more hydrophilic compounds that are more easily conjugated and excreted. In most mammals, including humans, family 1 enzymes such as CYP1A1, CYP1A2 and CYP1B1, are generally characterized by their metabolic ability to oxidize polycyclic aromatic hydrocarbons (*2*).

PCBs are poorly excreted from the body because of their high hydrophobicity. However, PCBs can be metabolized by hepatic drug-metabolizing P450s into their hydroxylated metabolites, leading to conjugation (*3*, *4*). Because of their low hydrophobicity, these metabolites can be more easily excreted than their parent compounds (*5*). Therefore, the types and amounts of drug-metabolizing P450s in a mammalian species largely determine the clearance and eventual toxicities of PCBs in that species.

CYP1A and 2B are important subfamilies for PCB metabolism. For example, 3,3′,4,4′- and 2,2′,5,5′-tetrachlorobiphenyls (TeCBs) are metabolized by rat P450s into their hydroxylated metabolites (*3*). However, the metabolism of 2,3′,4′,5-TeCB differs dramatically in mammals such as rats, guinea pigs and hamsters pretreated with phenobarbital or 3-methylcholanthrene (*6*). There are also some differences between humans and rats in the metabolism of mono- and dichlorinated dibenzo-*p*-dioxins by CYP1A1 and CYP1A2 (*7*). These results can be explained largely by differences in the concentrations of the enzymes in the liver and in the catalytic activity of each isoform. As expected, the toxicities of 2,3,7,8-tetrachlorodibenzo-*p*-dioxin (TCDD), the most toxic dioxin, vary widely among experimental animals (*8*). These species differences make it difficult, or even wrong, to extrapolate the exact toxicities of coplanar PCBs from animal studies to humans.

Highly chlorinated PCBs generally show higher hydrophobicity and persistence and have lower bioavailability and less reactivity in detoxification pathways than low chlorinated PCBs; there have been few studies of the metabolism of these PCBs by P450s.

Here, we used a combination of high-resolution gas chromatography and high-resolution mass spectrometry (HRGC/HRMS) to examine the metabolism of the most toxic and highly chlorinated PCB congener, 3,3′,4,4′,5-pentachlorobiphenyl (PCB126), by human and rat CYP1A1 enzymes. Moreover, we performed homology modelling of rat CYP1A1 and docking approach with PCB126 in an effort to explore the species differences in metabolism, and the preferred positions for hydroxylation.

Experimental Procedures

PCB

PCB126 was purchased from Cerilliant (Round Rock, TX, USA).

Preparation of microsomes

Recombinant *Saccharomyces cerevisiae* AH22/pAAH5 cells carrying the control vector, AH22/pYH1A1 cells expressing the human *CYP1A1* gene and AH22/pGYRr1A1 cells expressing the rat *CYP1A1* and yeast *NADPH-cytochrome P450 oxidoreductase* genes were pre-cultured in a synthetic minimum medium containing 8% glucose, 0.67% yeast nitrogen base without amino acids and 160 mg l^{-1} L-histidine at 30°C. The culture was then transferred to the medium containing 8% glucose, 1% yeast extract, 2% peptone and 40 mg l^{-1} adenine sulphate and incubated at 30°C to prepare the microsomal fractions. Microsomal fractions were prepared as described previously (*9*). Protein concentrations were measured by the Bradford method (*10*), using bovine serum albumin as a standard, and the levels of P450s were determined from the reduced CO difference spectra (*11*). The levels of human and rat CYP1A1 enzymes in the microsomes were 0.13 and 0.23 nmol mg^{-1} protein, respectively.

Measurement of catalytic activities of the Yeast microsomal fraction toward PCB126

The reaction mixture contained 0.77, 1.5, 3.1 or 6.1 μM PCB126 with a final concentration of dimethyl sulphoxide at 0.1%, microsomes containing 100 nM of either human and rat CYP1A1, 3.3 mM magnesium chloride and a NADPH regeneration system (5 mM glucose-6-phosphate and 1 U of glucose-6-phosphate dehydrogenase) in 100 mM potassium phosphate buffer at pH 7.4. This mixture was preincubated at 37°C, and the reaction was initiated by the addition of NADPH at a final concentration of 0.5 mM. After incubation for 2 h at 37°C and addition of ^{13}C-labelled hydroxylated PCB (OH-PCB) mixture (Wellington Laboratories Inc., Ontario, Canada) as an internal standard, the reactants were mixed twice with four volumes of hexane. The organic phase was collected and evaporated. Methylation of metabolites was then performed as described previously (*12*), and the residues were dissolved in ~100 μl of hexane.

Identification and quantification of OH-PCBs were performed by HRGC/HRMS in selective ion monitoring (SIM) mode by checking the isotope ratio ($[M]^+$:$[M+2]^+$) and fragment ions ($[M\text{-}CH_3Cl]^+$ and $[M\text{-}COCH_3]^+$), using synthesized and commercial standards as described previously (*13*). HRGC/HRMS was performed under conditions described previously (*13*).

Homology modelling

On the basis of the X-ray crystal structure of human CYP1A2 (*2*), we constructed a 3D model of human CYP1A1 (*14*). We used the 'Mutate monomers' tool in SYBYL Biopolymer (Tripos Inc., St Louis, MO, USA) to construct 3D models of rat CYP1A1 on the basis of the human CYP1A1 model. The side-chain conformations of all amino acid residues were retained from the template structure as much as possible. As mentioned in the 'Results' section, only one critical steric clash was observed in the Y263/F316 residues via the homology modelling, and the side-chain conformation of F316 was modified. Hydrogens were added to the structure by using SYBYL's internal tables for bond lengths and angles. Energy minimization of the constructed structure was performed until the energy gradient was lower than 0.1 kcal (mol Å)$^{-1}$ using the Tripos force field. The model structure was evaluated by using PROCHECK in the CCP4 program (*15*). Active-site volume was calculated by using MOLCAD application (*16*).

Substrate docking

Docking was performed using Surflex Dock in SYBYL 8.0 (Tripos). The human and rat CYP1A1 models were used as the CYP protein structure. The Surflex Dock (*17*) program uses an empirical scoring function to rank putative protein–ligand interactions by flexible docking of small molecules to protein structures. The scoring function includes hydrophobic interaction, polar interaction, steric crash, etc. and it has been updated and reparameterized with additional negative training data (*18*), together with a search engine that relies on a surface-based molecular similarity method (*19*). We applied the

'hard grid treatment' method of the Surflex Dock program, in which side chains of the active site residues are fixed. We obtained diverse substrate structure orientations for human and rat CYP1A1 enzymes, and selected substrate structures with the top 25 ranked by a weighted sum of scoring function described above.

Safety

This study was approved by the Committee for Safe Handling of Living Modified Organisms, at Kobe University (Permission number 17–98), and was performed in accordance with the Guidelines of the Committee.

Results

Catalytic activities of rat CYP1A1 toward PCB126

Two peaks were observed in the chromatograph of the molecular weights of methylated mono hydroxylated tetrachlorobiphenyl (MeO-TeCB) and methylated mono hydroxylated pentachlorobiphenyl (MeO-PeCB) in the presence of microsomes containing rat CYP1A1 and NADPH (Fig. 1I and J). These peaks also matched the isotope ratios ($[M]^+$:$[M+2]^+$) of MeO-TeCB and MeO-PeCB, meaning that the peaks were from tetra- and pentachlorinated compounds, respectively (Supplementary Fig. S1). The results indicated that the peaks were from mono hydroxylated TeCB (OH-TeCB) and mono hydroxylated PeCB (OH-PeCB); their retention times were ~25.4 and 31.5 min, respectively. Comparison with the retention times of the authentic standards (Fig. 1A and B) indicated that PCB126 was metabolized by rat CYP1A1 into 4-OH-3,3′,4′,5-TeCB and 4-OH-3,3′,4′,5,5′-PeCB (Fig. 2); the patterns of the fragment ions, which were both $[M\text{-}COCH_3]^+$, showing that the substituted OH group was at the *meta* or *para* position (*12*), did not conflict with those of the corresponding metabolites (Supplementary Fig. S2). The production of 4-OH-3,3′,4′,5,5′-PeCB was accompanied by migration of a chlorine atom, and this migration was often observed in metabolisms of PCBs and named NIH shift (*3*). The peak of 4-OH-3,3′,4′,5-TeCB was much larger than that of 4-OH-3,3′,4′,5,5′-PeCB. The kinetic parameters of rat CYP1A1 for 4-OH-3,3′,4′,5-TeCB were investigated by using the Michaelis–Menten equation and Lineweaver–Burk plot (Fig. 3, Table I). The saturation curve fitted the Michaelis–Menten equation very well (Fig. 3A); the *R*-value was more than 0.99, showing that the data sets were very reliable. From the Lineweaver–Burk plots, the values of K_m to PCB126 (the binding affinity), V_{max} (the catalytic activity) and V_{max}/K_m were 1.57 μM, 0.0367 pmol product min^{-1} (nmol P450)$^{-1}$, and 0.0233, respectively.

These peaks were not detected under the same conditions without NADPH (Fig. 1G and H), indicating that peak formation depended on rat CYP1A1 activity. Under the same conditions, microsomes containing human CYP1A1 and the control vector microsomes, metabolized PCB126 to less than the detection limit or not at all, regardless of the presence of NADPH (Fig. 1C–F, Supplementary Fig. S3).

3D structures of human and rat CYP1A1 enzymes

To clarify the mechanisms behind these differences in catalytic activity, we attempted to construct a homology model of rat CYP1A1. We successfully obtained a 3D structure of rat CYP1A1 enzyme by using human CYP1A1 as a base model; A Ramachandran plot showed that 99.4% of the residues in rat CYP1A1 was in either the most favored or allowed regions. The rat CYP1A1 model was quite similar to human CYP1A1. The result was consistent with the high sequence identity (79%) between human and rat CYP1A1 proteins. Twenty residues involved in the substrate-binding cavity were identified, and only four residues were not conserved between human (S116, S122, N221 and L312) and rat (A120, T126, S225 and F316) CYP1A1 proteins (Table II). These residues might play an important role in the specific hydroxylation of PCB126.

After executing the 'Mutate monomers' function, we found one serious steric crush error between Y263 on the G-Helix and F316 on the I-Helix in rat CYP1A1 (Fig. 4A and B). Therefore, we modified the side chain conformation of F316 from $\chi_1 - 60^\circ$ to $\chi_1 180^\circ$. This conformation was favorable in rat CYP1A1, because the amino acid residue corresponding to S116 in human CYP1A1 was A120; this made extra space to accommodate the side chain of F316. Consequently, the phenyl group protruded into the substrate binding cavity and made the cavity volume smaller (510 $Å^3$) than that of human CYP1A1 (600 $Å^3$) (Fig. 4A and B). The volumes of both active sites were larger than that of CYP1A2 (470$Å^3$) (*14*). The geometry of the cavities also differed. Importantly, the cavity of rat CYP1A1 was narrower but still kept its shape to accommodate planar substrates.

Docking model approach

To verify the details of the interaction of each CYP with PCB126, we performed a docking study of PCB126 with each CYP. We obtained diverse PCB126 complex structures for each CYP1A1, from which we selected the PCB126 orientations with the top 25 ranked by the scoring function, because they covered all the representative locations of PCB126. Figure 4A and B show the distinct orientations of PCB126 for each CYP; the structures could be classified into 13 binding structures toward human CYP1A1 (Fig. 4A) and 7 towards rat CYP1A1 (Fig. 4B). Human CYP1A1 could accommodate PCB126 with multiple orientations, and all of these were positioned >7 Å away from the iron atom of the haem. In contrast, although rat CYP1A1 could accommodate PCB126 with fewer orientations, all of them were clearly oriented to the haem iron. No π–π orbital interaction was observed between F316 and the substrate, and these orientations were not affected by such interaction. Some were located close enough to the haem iron—less than 6 Å—to be metabolized (*20*). The preferred position for hydroxylation, which is closest to the haem iron, was the 4 position of carbon. Orientations in which the dichlorinated phenyl ring was directed towards the haem were possible, but 4′ position of carbon was more distant from the iron than the reverse orientation, because the chlorine atoms of the trichlorinated phenyl ring conflicted with F316 when the opposite ring became close to the iron. In

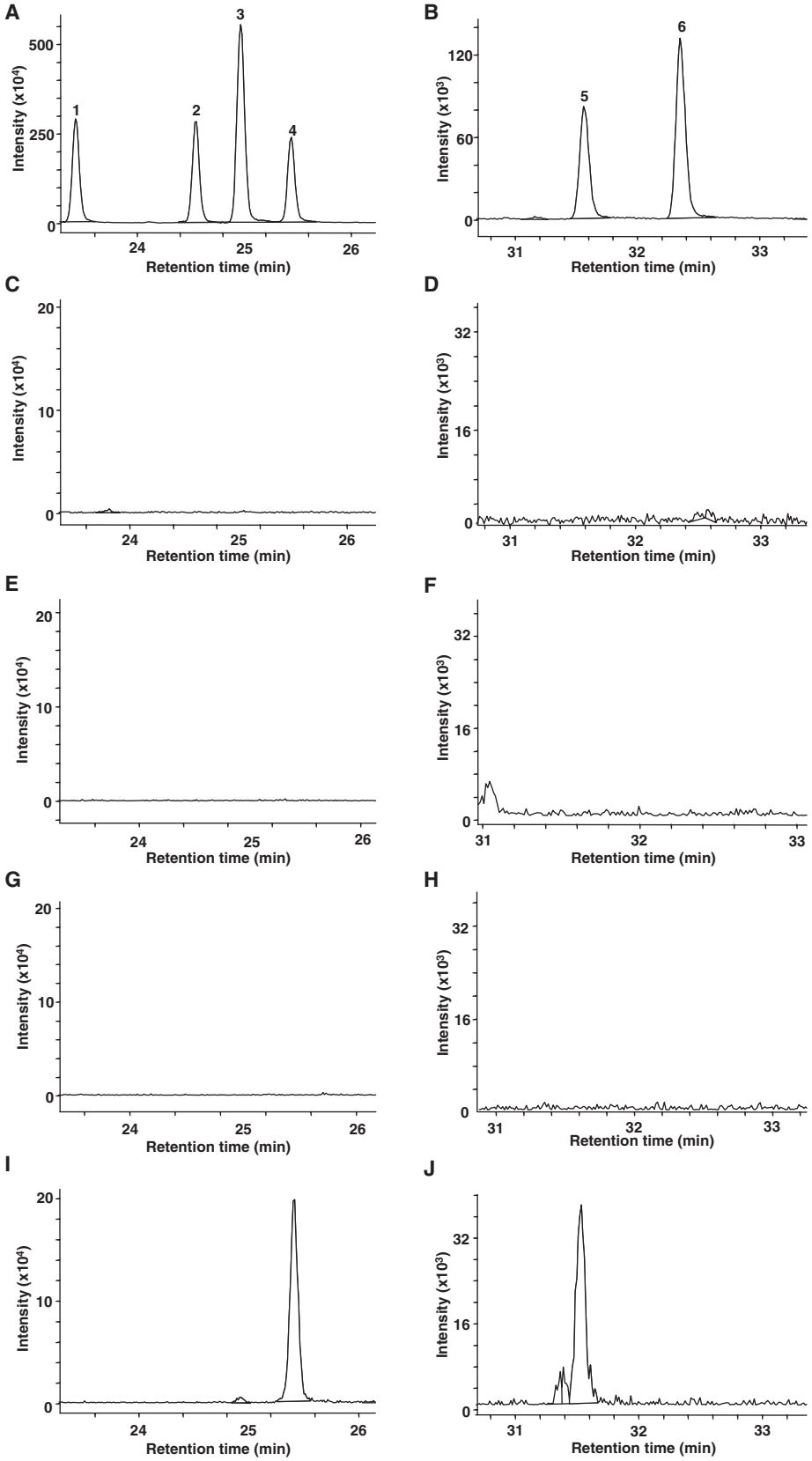

Fig. 1 HRGC/HRMS analyses of MeO-TeCBs (A, C, E, G and I) and MeO-PeCBs (B, D, F, H and J) in metabolism of PCB126 by human and rat CYP1A1 enzymes. The microsomes containing 100 nM of either human and rat CYP1A1 were incubated in the reaction mixture with 6.1 μM PCB126 for 2 h. The extracted metabolites were quantified by HRGC/HRMS. (A and B) show the authentic standards: Peak 1, 3-MeO-2′,3′,4′,5′-TeCB; peak 2, 4-MeO-2,3′,5,5′-TeCB; peak 3, 4-MeO-2′,3′,4′,5′- and 4-MeO-2,3′,4′,5-TeCB; peak 4, 5-MeO-2,3′,4,4′- and 4-MeO-3,3′,4′,5-TeCB; peak 5, 4-MeO-3,3′,4′,5,5′-PeCB; peak 6, 4-MeO-2′,3,3′,4′,5′-PeCB. (C and D), (E and F) and (I and J) show the results for vector alone (control), human and rat CYP1A1 enzymes with NADPH, respectively. (G and H) show the results for rat CYP1A1 enzyme without NADPH.

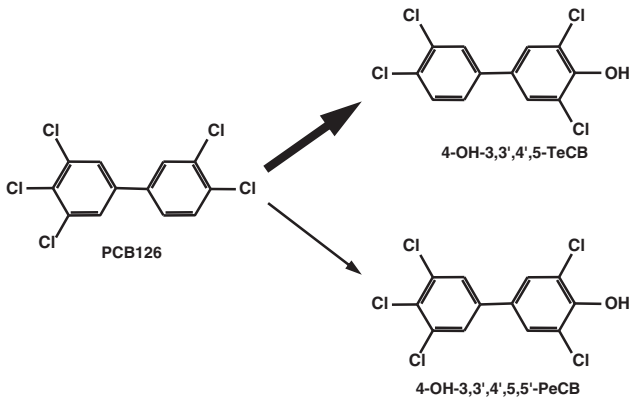

Fig. 2 Proposed metabolic pathways of PCB126 by rat CYP1A1.

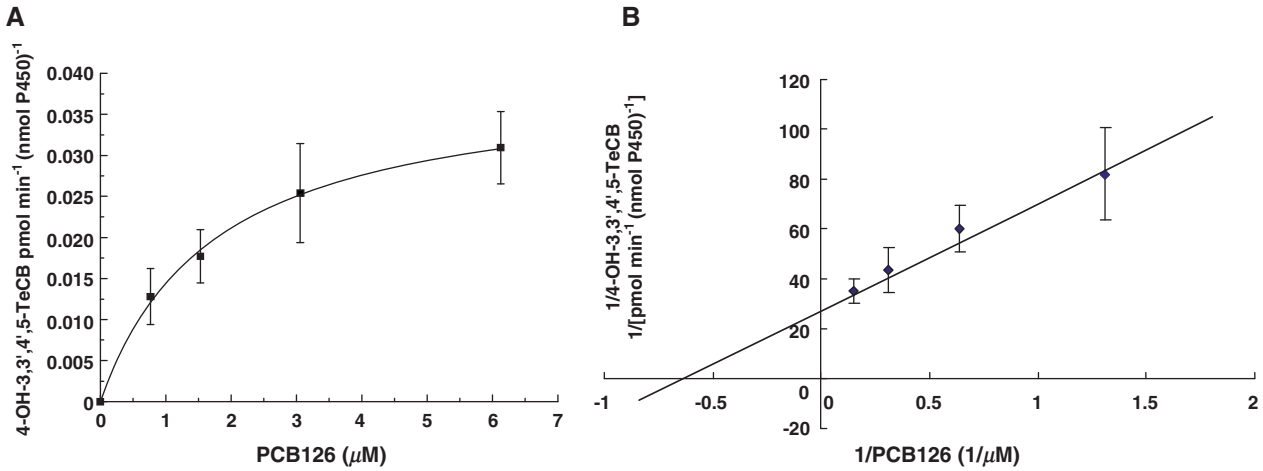

Fig. 3 Michaelis–Menten (A) and Lineweaver–Burk (B) plots of kinetics of rat CYP1A1 to 4-OH-3,3′,4′,5-TeCB. The microsomes containing 100 nM of rat CYP1A1 were incubated in the reaction mixture with 0.77, 1.5, 3.1 or 6.1 μM PCB126 for 2 h. The extracted metabolite of 4-OH-3,3′,4′,5-TeCB was quantified by HRGC/HRMS. All values were means ± standard deviation of five separate experiments.

Table I. Kinetic parameters of CYP1A1s for hydroxylation of PCB126 into 4-OH-3,3′,4′,5-TeCB as determined by Lineweaver–Burk plot.

CYP1A1	K_m	V_{max}	V_{max}/K_m
Human	ND	ND	–
Rat	1.57	0.0367	0.0233

The microsomes containing 100 nM of rat CYP1A1 were incubated in the reaction mixture with 0.77, 1.5, 3.1 or 6.1 μM PCB126 for 2 h. The extracted metabolite of 4-OH-3,3′,4′,5-TeCB was quantified by HRGC/HRMS. K_m is given in μM and V_{max} is given in pmol product min^{-1} (nmol P450)$^{-1}$. ND, not detected.

the docking models, the closest distance between the iron and the 4 position of the carbon atom of PCB126 was 7.3 Å in human CYP1A1 and 4.7 Å in rat CYP1A1 (Fig. 4C and D). Rat CYP1A1 showed that the angle between the four position of the carbon atom in PCB126 and the haem was 70°.

Discussion

Substrate affinities, metabolic activities and the preferred positions of hydroxylation of the same P450 species differ widely among organisms. One of the reasons is that the size and shape of the cavities are different, even if the amino acid residues in the substrate binding domains that affect the substrate configurations do not differ greatly.

In studies of the metabolism of chlorinated aromatic hydrocarbons, rat CYP1A1 showed higher catalytic activity for highly chlorinated congeners than did human CYP1A1 (*21*). Among PCBs, PCB126 has received great interest because of its toxicity, as determined by the World Health Organization (WHO) (*22*), and *in vivo* studies have indicated that PCB126 could be biotransformed into hydroxylated metabolites in rats (*5*). However, few *in vitro* studies of this metabolism, or of the identification of the enzymes responsible, have been reported, probably because the activity and detection limits of the analytical devices have been too low to detect and quantify the metabolites. We therefore employed the SIM mode of HRGC/HRMS. Our results were very consistent with those of the above mentioned previous reports. However, no structural evidence explaining these differences had been revealed, and the mechanism was still unclear. One of the reasons is that the X-ray crystal structure of CYP1A1 species has not yet been revealed.

On the other hand, the X-ray crystal structure of CYP1A2 has recently been reported in a first analysis of the CYP1A family (*2*). This enables more exact homology modelling of the CYP1A family as a whole because of the highly preserved structures of its members (*23*). Therefore, we performed homology modelling of human (*14*) and rat CYP1A1 enzymes and studied a PCB126 docking model to clarify the mechanism.

Table II. Residues involved in substrate-binding cavities of human and rat CYP1A1 enzymes indicated by the homology modelling.

Human	Rat	SRS location	Secondary structure
I115	I119	SRS1	Loop
S116	*A120*	*SRS1*	*Loop*
S120	S124	SRS1	Loop
S122	*T126*	*SRS1*	*Loop*
F123	F127	SRS1	Loop
N221	*S225*	*SRS2*	*F-helix*
F224	F228	SRS2	F-helix
G225	G229	SRS2	F-helix
L254	L258	SRS3	G-helix
F258	F262	SRS3	G-helix
L312	*F316*	*SRS4*	*I-helix*
D313	D317	SRS4	I-helix
G316	G320	SRS4	I-helix
A317	A321	SRS4	I-helix
D320	D324	SRS4	I-helix
T321	T325	SRS4	I-helix
V382	V386	SRS5	Loop
I386	I390	SRS5	Loop
L496	L500	SRS6	Loop
T497	T501	SRS6	Loop

Different residues between human and rat are italicized.

In the substrate binding cavity, four out of the 20 residues were not conserved. Interestingly, the modelling results strongly suggested that although, in rat CYP1A1, residues T126 and S225 contributed less to modification of the substrate binding cavity than the other residues, residues A120 and F316 in rat CYP1A1 together made the cavity much narrower than in human CYP1A1 because of the conflict of residues Y263 and F316 and the finding that A120 allowed F316 to flip. However, rat CYP1A1, with its narrow cavity, had greater catalytic activity for PCB126 than human CYP1A1, with its wide cavity. The finding that α-naphthoflavone (a P450 inhibitor) and 2,3,7,8-TCDD can be accommodated easily or tightly, but not metabolized, by human CYP1A2 and CYP1A1, respectively, supports the low catalytic activity of human CYP1A1 for PCB126 (*2*, *24*). The two residues responsible for the narrowed cavity therefore play an important role in the metabolism of PCB126 by rat CYP1A1.

The results of the docking study indicate that rat CYP1A1 possesses a cavity wide enough to accommodate PCB126. The projection of F316 into the cavity will raise the probability of metabolism of PCB126. The preferred position for hydroxylation is also consistent with the structure of the metabolites. The results of the modelling and docking study also suggest that human CYP1A1 is able to accommodate PCB126 more easily than can rat CYP1A1. However, it will not offer sufficient and maintained closeness between PCB126 and the haem iron atom as observed in rat CYP1A1. This is consistent with our lack of detection of metabolites in the case of human CYP1A1. The results of the metabolism and modelling and docking studies therefore complement each other.

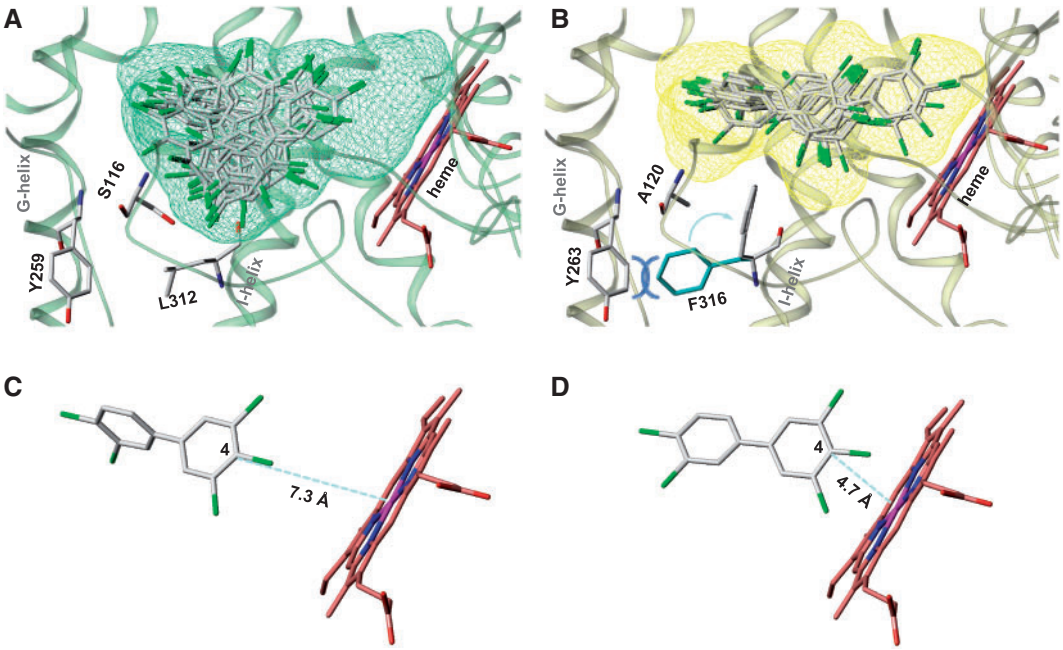

Fig. 4 PCB126 docked into substrate binding cavity of human (A and C) and rat (B and D) CYP1A1 enzymes. 3D model of rat CYP1A1 was constructed with the basis of the previously reported human CYP1A1 model using 'Mutate monomers' tool in SYBYL Biopolymer. Docking was performed using Surflex Dock in SYBYL 8.0. The Connolly channel surfaces of the cavities are displayed by colored mesh. (A) L312 faced Y259, but not the substrate binding cavity. (B) Because of steric hindrance with Y263, F316 was oriented towards the substrate binding cavity. The closest PCB126 to the iron atom in (A) and (B) is shown in (C) and (D), respectively.

Moreover, both residues A120 and F316, seen in rat CYP1A1, are rare in human CYP1A1 and in other well-studied mammalian CYP1A1 enzymes (dog, golden hamster, guinea pig, monkey, mouse and rabbit), although the tyrosine residue causing the conflict is well conserved or is replaced by similar-sized residues, except in guinea pig CYP1A1 (Supplementary Fig. S4). Furthermore, a rat with an F316A mutation of CYP1A1, which should have formed a larger cavity, showed less catalytic activity toward PCDD than the wild-type (T. Sakaki, personal communication). These findings suggest that a large residue such as F316 can co-exist only with the smallest residue, A120, and that the cavity shape and catalytic activity of rat CYP1A1 may be unique.

The metabolites of dioxins and coplanar PCBs probably show less toxicity and better clearance than the parent compound in mammals, perhaps because AhR affinity and hydrophobicity decline with dechlorination and hydroxylation. The affinity of 8-hydroxy-2,3,7-trichlorodibenzo-*p*-dioxin (TriCDD) for the AhR was <0.001% of that of 2,3,7,8-TCDD and 10% of that of 2,3,7-TriCDD (*25*). The metabolite 4-OH-3,3′,4′,5-TeCB shows much less toxicity and accumulation than the parent PCB126 in exposed rats (*5*). These findings and our results strongly suggest that PCB126 is more toxic and bio-accumulative in humans than in rats. Toxic equivalence factors (TEFs) of each congener of dioxins and coplanar PCBs have been defined through estimation, largely on the basis of *in vivo* studies in animals by WHO, as relative toxicities to 2,3,7,8-TCDD (*22*). In this paper, instead of 2,3,7,8-TCDD (TEF = 1), PCB126 (TEF = 0.1) was indeed used in rat studies as a reference compound, meaning that the metabolism activity of PCB126 in rats must be the same as that in humans. Therefore, nothing is considered on species differences, whereas PCB126 is metabolized by rat CYP1A1 but not by human CYP1A1. In mice studies, since the species differences are considered because of the unique low induction of drug-metabolizing enzymes by PCB126, it was concluded that PCB126 may be inappropriate as a reference compound. Our results suggest that PCB126 is not appropriate as a reference compound in rat studies since CYP1A1 activity in the rat is also unique to be able to metabolize PCB126.

Therefore, when the toxicities of congeners metabolized by rat toward humans are estimated from rat studies, they may be underestimated; overestimation may occur not only in the opposite situation but also when PCB126 is used as a reference in the studies. Moreover, OH-PCBs are considered to behave as endocrine disruptors. They can bind more strongly than PCBs, including PCB126, to the serum thyroid hormone binding protein transthyretin, displacing the natural ligand thyroxine (*26*). 4-OH-PCBs, including 4-OH-3,3′,4′,5-TeCB and 4-OH-3,3′,4′,5,5′-PeCB, show greater thyroid hormonal and estrogenic activities by binding to the thyroid hormone and estrogen receptors than do PCBs; PCB126 does not bind to the thyroid hormone receptor (*26*, *27*). PCB metabolism is therefore thought to decrease AhR-mediated toxicity but to cause other toxicities, and extrapolation of the results of such *in vivo* studies in the rat to humans must be done carefully.

The rat is therefore not always a suitable animal for estimating effects in humans, such as the toxicities of dioxins and dioxin-like compounds, the carcinogenicity of active intermediates and the potency of drugs, at least if they are metabolized by CYP1A1.

Supplementary Data

Supplementary Data are available at *JB* Online.

Acknowledgements

We thank Ms Tomomi Matsui and Miku Yabu of Kobe University for their technical assistance.

Funding
Ministry of Agriculture, Forestry and Fisheries of Japan (Hazardous Chemicals HC-06-2311-1 to H.I.; Genomics for Agricultural Innovation GMB-0006 to H.I.).

Conflict of interest
None declared.

References

1. Bock, K.W. and Kohle, C. (2006) Ah receptor: dioxin-mediated toxic responses as hints to deregulated physiologic functions. *Biochem. Pharmacol.* **72**, 393–404
2. Sansen, S., Yano, J.K., Reynald, R.L., Schoch, G.A., Griffin, K.J., Stout, C.D., and Johnson, E.F. (2007) Adaptations for the oxidation of polycyclic aromatic hydrocarbons exhibited by the structure of human P450 1A2. *J. Biol. Chem.* **282**, 14348–14355
3. Ishida, C., Koga, N., Hanioka, N., Saeki, H.K., and Yoshimura, H. (1991) Metabolism *in vitro* of 3,4,3′,4′- and 2,5,2′,5′-tetrachlorobiphenyl by rat liver microsomes and highly purified cytochrome P-450. *J. Pharmacobio-Dyn.* **14**, 276–284
4. Sacco, J.C. and James, M.O. (2004) Glucuronidation in the polar bear (*Ursus maritimus*). *Mar. Environ. Res.* **58**, 475–479
5. Koga, N., Beppu, M., and Yoshimura, H. (1990) Metabolism *in vivo* of 3,4,5,3′,4′-pentachlorobiphenyl and toxicological assessment of the metabolite in rats. *J. Pharmacobio-Dyn.* **13**, 497–506
6. Koga, N., Kikuichi, N., Kanamaru, T., Kuroki, H., Matsusue, K., Ishida, C., Ariyoshi, N., Oguri, K., and Yoshimura, H. (1998) Metabolism of 2,3′,4′,5-tetrachlorobiphenyl by cytochrome P450 from rats, guinea pigs and hamsters. *Chemosphere* **37**, 1895–1904
7. Shinkyo, R., Sakaki, T., Ohta, M., and Inouye, K. (2003) Metabolic pathways of dioxin by CYP1A1: species difference between rat and human CYP1A subfamily in the metabolism of dioxins. *Arch. Biochem. Biophys.* **409**, 180–187
8. Neal, R.A. (1985) Mechanisms of the biological effects of PCBs, polychlorinated dibenzo-*p*-dioxins and polychlorinated dibenzofurans in experimental animals. *Environ. Health Perspect.* **60**, 41–46
9. Oeda, K., Sakaki, T., and Ohkawa, H. (1985) Expression of rat liver cytochrome P-450MC cDNA in *Saccharomyces cerevisiae*. *DNA* **4**, 203–210
10. Bradford, M.M. (1976) A rapid and sensitive method for the quantitation of microgram quantities of protein

utilizing the principle of protein-dye binding. *Anal Biochem*. **72**, 248–254
11. Omura, T. and Sato, R. (1964) The carbon monoxide-binding pigment of liver microsomes. I. Evidence for its hemoprotein nature. *J. Biol. Chem*. **239**, 2370–2378
12. Sakiyama, T., Yamamoto, A., Kakutani, N., Fukuyama, J., and Okumura, T. (2007) Hydroxylated polychlorinated biphenyls (OH-PCBs) in the aquatic environment: levels and congener profiles in sediments from Osaka, Japan. *Organohalogen Compd*. **69**, 1380–1383
13. Suzuki, M., Takemine, S., Tsurukawa, M., Matsumura, C., Nakano, T., and Imaishi, H. (2009) Investigation of hydroxylated polychlorinated biphenyls (OH-PCBs) in the air and the sediments around the paper recycling plant. *Organohalogen Compd*. **71**, 1881–1885
14. Itoh, T., Takemura, H., Shimoi, K., and Yamamoto, K. (2010) A 3D model of CYP1B1 explains the dominant 4 hydroxylation of estradiol. *J. Chem. Inf. Model*. **50**, 1173–1178
15. The CCP4 suite. (1994) Programs for protein crystallography. *Acta. Crystallogr. D Biol. Crystallogr*. **50**, 760–763
16. Brickmann, J., Exner, T.E., Keil, M., and Marhöfer, R.J. (2000) Molecular graphics – trends and perspectives. *J. Mol. Mod*. **6**, 328–340
17. Ruppert, J., Welch, W., and Jain, A.N. (1997) Automatic identification and representation of protein binding sites for molecular docking. *Protein Sci*. **6**, 524–533
18. Pham, T.A. and Jain, A.N. (2006) Parameter estimation for scoring protein-ligand interactions using negative training data. *J. Med. Chem*. **49**, 5856–5868
19. Jain, A.N. (2000) Morphological similarity: a 3D molecular similarity method correlated with protein-ligand recognition. *J. Comput. Aided. Mol. Des*. **14**, 199–213
20. Sykes, M.J., McKinnon, R.A., and Miners, J.O. (2008) Prediction of metabolism by cytochrome P450 2C9: alignment and docking studies of a validated database of substrates. *J. Med. Chem*. **51**, 780–791
21. Shinkyo, R., Sakaki, T., Ohta, M., and Inouye, K. (2003) Metabolic pathways of dioxin by CYP1A1: species difference between rat and human CYP1A subfamily in the metabolism of dioxins. *Arch. Biochem. Biophys*. **409**, 180–187
22. Van den Berg, M., Birnbaum, L.S., Denison, M., De Vito, M., Farland, W., Feeley, M., Fiedler, H., Hakansson, H., Hanberg, A., Haws, L., Rose, M., Safe, S., Schrenk, D., Tohyama, C., Tritscher, A., Tuomisto, J., Tysklind, M., Walker, N., and Peterson, R.E. (2006) The 2005 World Health Organization reevaluation of human and mammalian toxic equivalency factors for dioxins and dioxin-like compounds. *Toxicol. Sci*. **93**, 223–241
23. Lewis, B.C., Mackenzie, P.I., and Miners, J.O. (2007) Comparative homology modeling of human cytochrome P4501A1 (CYP1A1) and confirmation of residues involved in 7-ethoxyresorufin *O*-deethylation by site-directed mutagenesis and enzyme kinetic analysis. *Arch. Biochem. Biophys*. **468**, 58–69
24. Inouye, K., Shinkyo, R., Takita, T., Ohta, M., and Sakaki, T. (2002) Metabolism of polychlorinated dibenzo-*p*-dioxins (PCDDs) by human cytochrome P450-dependent monooxygenase systems. *J. Agric. Food. Chem*. **50**, 5496–5502
25. Sakaki, T., Shinkyo, R., Takita, T., Ohta, M., and Inouye, K. (2002) Biodegradation of polychlorinated dibenzo-*p*-dioxins by recombinant yeast expressing rat CYP1A subfamily. *Arch. Biochem. Biophys*. **401**, 91–98
26. Cheek, A.O., Kow, K., Chen, J., and McLachlan, J.A. (1999) Potential mechanisms of thyroid disruption in humans: interaction of organochlorine compounds with thyroid receptor, transthyretin, and thyroid-binding globulin. *Environ. Health Perspect*. **107**, 273–278
27. Kitamura, S., Jinno, N., Suzuki, T., Sugihara, K., Ohta, S., Kuroki, H., and Fujimoto, N. (2005) Thyroid hormone-like and estrogenic activity of hydroxylated PCBs in cell culture. *Toxicology* **208**, 377–387